Side-Use of a Ge p-i-n Photo Diode for Electrical Application in a Photonic BiCMOS Technology

S. Lischke, D. Knoll, S. Tolunay-Wipf, C. Wipf, C. Mai, A. Fox, F. Herzel, and M. Kaynak

IHP, Im Technologiepark 25, 15236 Frankfurt (Oder), Germany

lischke@ihp-microelectronics.com

Abstract— **In this paper we demonstrate the potential use of a germanium p-i-n diode, available without additional processing effort in a photonic BiCMOS technology, for electronic applications. A cut-off frequency above 400 GHz was obtained by S-parameter measurements without any certain design optimization of the diode. The device construction on SOI yields in the isolation of the diode from the substrate. Moreover, the lateral current flow enables low series resistance for the diode. Potential applications are antenna-switching or mixers.**

Keywords— BiCMOS; Ge p-i-n diode; Silicon photonics

I. INTRODUCTION

Integration of Si-photonics with electronics, which is a key towards complex receiver and transmitter devices for future communication applications, has already been realized with different technological approaches [1–4]. Out of these, photonics integration in the frontend-of-line (FEOL) of an integrated circuit technology [3, 4] allows for shortest possible photonics to electronics interconnects from which high-speed performance of electronic-photonic integrated circuits (ePIC) can greatly benefit.

Heterogeneously integrated transmitters [3] and transceivers [4] were already proposed indicating feasibility of 100 Gb/s single-channel data rates based on cost-saving silicon-only technology. High-performance SiGe BiCMOS technology was chosen in both cases as electronic baseline process for fabricating the analog frontend circuitry because it outperforms highly scaled CMOS in terms of combined RF performance, breakdown voltage and costs.

The integration scheme of IHP's electronic-photonic integrated circuit technology enables for the first time for monolithically integrated Si-based transceivers by combining segmented Mach-Zehnder-Interferometer (MZI) modulators and high-speed germanium photo detectors with a BiCMOS core. The bipolar module of choice for IHP's first ePIC process foundry offers SiGe HBTs with f_T/f_{max} of about 200 GHz [5].

Moreover, by the integration of the particular modules for the photonic functionality, this process potentially enables the side-use of photonic devices in order to extend the overall device portfolio. Here, we present first results of the pure electrical performance of a germanium p-i-n diode, which is completely isolated from the substrate by being located on SOI, hampered for most Schottky-barrier diodes (SBD) implementations, where a vertical current flow usually is required for high-speed performance. So far, the germanium p-i-n diode was exclusively used as photo detector and optimized in that manner [6]. However, the integration scheme allows for the independent optimization of the diode for opto-electrical and the pure electrical side-use purpose.

II. PHOTONIC BICMOS PROCESS

IHP's ePIC process and its main features have previously been described in detail [5]. Meanwhile, the process was demonstrated with improved SiGe HBTs and Ge photo detectors offering 70 GHz opto-electrical bandwidth and high responsivity of about 1 A/W, e.g. facilitating the fabrication of coherent receivers with high sensitivity [2].

The photonic BiCMOS technology utilizes the local-SOI approach [7] that allows us to reconcile the fundamentally differing substrate requirements of photonics (SOI) and high-speed BiCMOS (bulk), enabling for the realization of state-of-the-art photonic devices at the same time with a low-ohmic collector formation, mandatory for high-performance HBTs. Fig. 1 shows TEM cross-sections illustrating the Ge photo detector integration with BiCMOS and essential diode features, respectively. The diode is fabricated from a Ge layer, selectively grown on a Si waveguide (Si-WG). A detailed process flow description is available elsewhere [5].
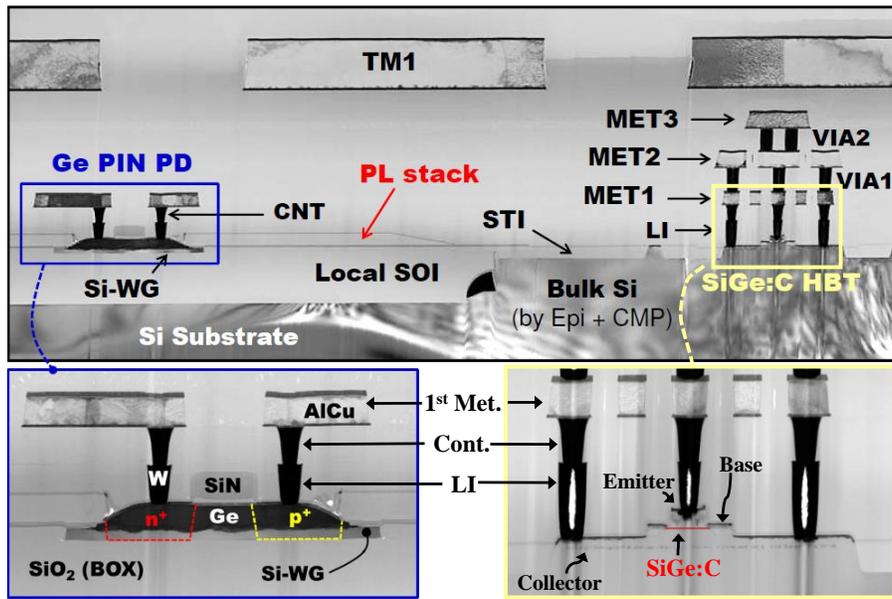
Fig. 1: TEM cross-sections of a Ge photodiode on SOI and a SiGe:C HBT fabricated in an adjacent bulk region (above). Details of the Ge lateral p-i-n photodiode can be seen on the bottom left. Diode cross-section is perpendicular to the direction of light incidence. The photodiode is evanescently coupled to a silicon waveguide. A detailed cross-section of the SiGe HBT is seen on the bottom right.

Various demonstrator circuits fabricated in IHP's photonic BiCMOS technology have already been presented, proving the achieved status of photonic BiCMOS process development and its suitability for the realization of transceiver systems at high data rates:

1) Monolithically integrated receivers for 25 Gbps [8] and 40 Gbps [9] as well as a single polarization QPSK receiver for 56 Gbps (28 Gbaud) [10] demonstrate the potential of the ePIC approach on the receiver side.

2) Monolithically integrated transmitters demonstrating high extinction ration of 13 dB with data rate of 28 Gb/s [11] were presented, allowing in combination with high-speed receivers for the realization of Si-based, monolithically integrated transceivers with data rates towards 400 Gbps [12].

III. EXPERIMENTS

The fabrication of the germanium photo detectors basically allows for the realization of diodes with two different contact schemes. In a first diode generation, tungsten plugs land on a silicon cap of some tens of nanometers on top of the germanium (Fig. 2, left) [13]. In this structure, the p^+ and n^+ doped Ge regions have a similar width or even wider compared to the width "X" (Fig. 4). This approach was found to limit the detector performance in the manner of the opto-electric frequency response but also the responsivity [6]. In a revised detector construction, the tungsten plugs land on silicon-offshoots aside the germanium (Fig. 2, right), enabling significantly increased responsivity at the same time with strongly increased frequency response behavior. Here, the p^+ and n^+ doped Ge regions were narrowed and are about 2x smaller than the width "X". The improvement in the frequency behavior can be attributed to the changed ratio between the photo carriers generated in high-field and non-depleted Ge regions [14].

Both types of germanium photo detector constructions solely differ in their layout and can thus be realized in the same process flow. Owing to the changed contact scheme for the diode construction where the tungsten plugs land aside the germanium, the series resistance noticeably increases referring to the version where the contacts land on top of the diode. However, the new construction yields in higher opto-electrical bandwidths, as the photo detectors are not limited by the charging time (RC).
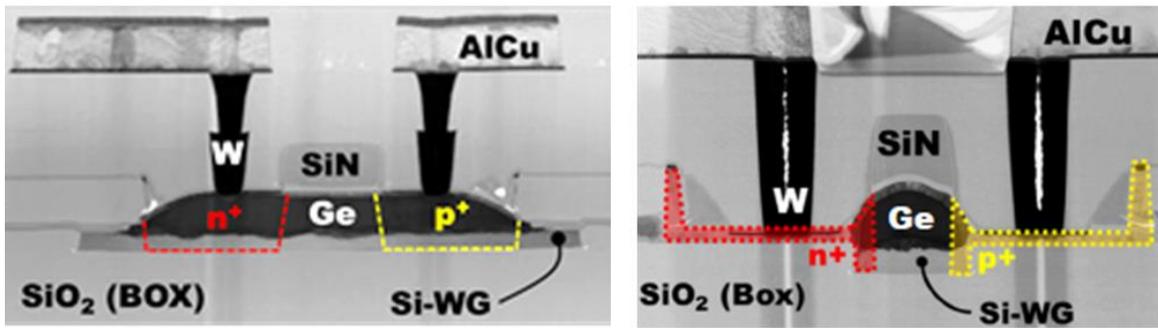
Fig. 2: Cross sections of Ge p-i-n photodiodes: first diode generation (wide p^+/n^+, left) and new design (narrow p^+/n^+, right). Cuts perpendicular to the direction of light incidence when used as photo detector.

In contrast to a SBD, the realization of lateral germanium p-i-n diodes on SOI enables a fully isolation from the substrate at the same time maintaining low resistance.

An adaptation of a usual vertical SBD on SOI would inevitably lead to increased resistances, evoked by the top silicon layer with a thickness of only 220 nm, which is given by the SOI substrate used for the photonic devices in IHP's ePIC process.

The current-voltage characteristics for both photo detector construction types are illustrated in Fig. 3. Here, the green-curve ("wide p^+/n^{+}") refers to the diode shown in Fig. 2 on the left, and the blue curve ("narrow p^+/n^{+}") belongs to the new diode design shown in Fig. 2 on the right hand side [6].
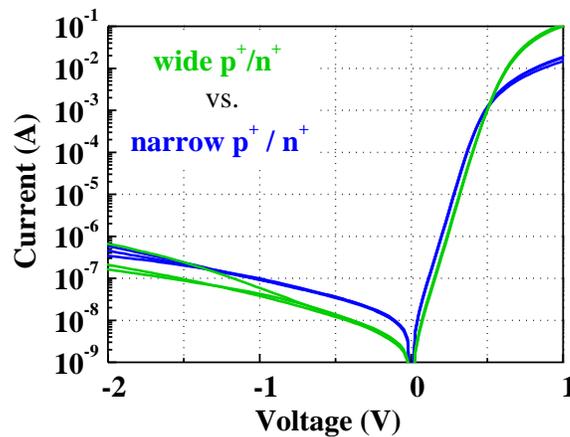

Fig. 3: Room temperature DC characteristics characteristics for the two diode construction types at a fixed depletion layer width "X". Diodes were measured on 3 dies.

Clearly, in applications as switching the resistance of the germanium p-i-n diode might become a crucial parameter. Thus, only the diode construction type with tungsten plugs from the top (Fig. 2 on the left, wide p^+/n^+) is taken into account for the investigations of the switching capabilities. Out of this consideration, two design variations of the first diode generation will be discussed as follows. As illustrated in Fig. 4, the width of the depletion layer that is controlled by the width of silicon-nitride (SiN) pedestal "X" has been varied. Limited by existing designs, only two variants were available for first investigations.
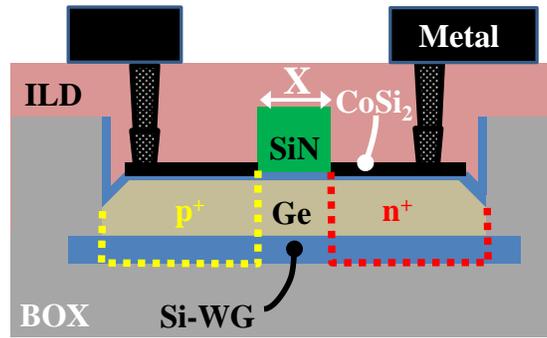
Fig. 4: Diode construction type with tungsten contacts landing on top of the germanium: width X is varied by design (width of the SiN-pedestal that facilitates the alignment during ion-implantation for p- and n-doping).

IV. RESULTS AND DISCUSSION

Diode C-V characteristics for two SiN-pedestal widths, $X_1 = 600$ nm and $X_2 = 800$ nm, extracted from small signal measurements, are presented in Fig. 5. Note, that in account to the phosphorous diffusion in germanium, the width "X" does not represent the actual depletion layer width after the full process.
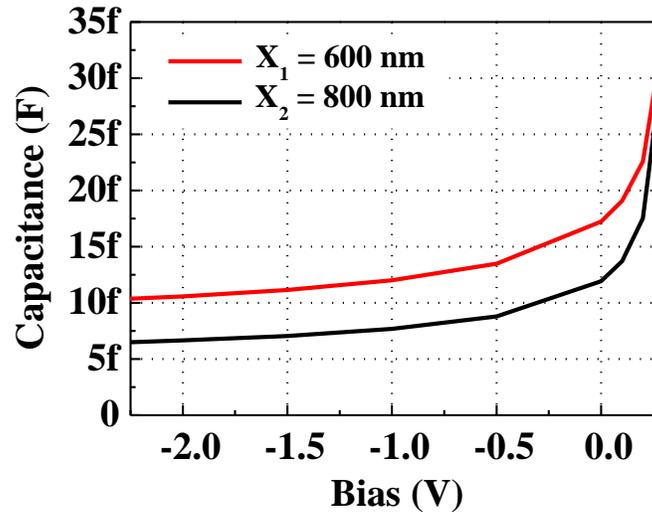

Fig. 5: Capacitance vs. voltage for two layout variations extracted from small signal measurements.

The corresponding resistances, extracted from small signal measurements, for both diodes ($X_1 = 600$ nm and $X_2 = 800$ nm) are presented in Fig. 6. First of all, substantial differences for the capacitance and resistance become obvious. As expected, the capacitance increases with decreasing width of the depletion layer. Here, a decrease of the SiN-pedestal width (from X_2 to X_1) causes a capacitance increase of about 50 % at 0 V. On the other hand, the decreasing depletion layer width leads to a significantly decreased resistance values, especially around 0 V (the resistance drops to about a third).
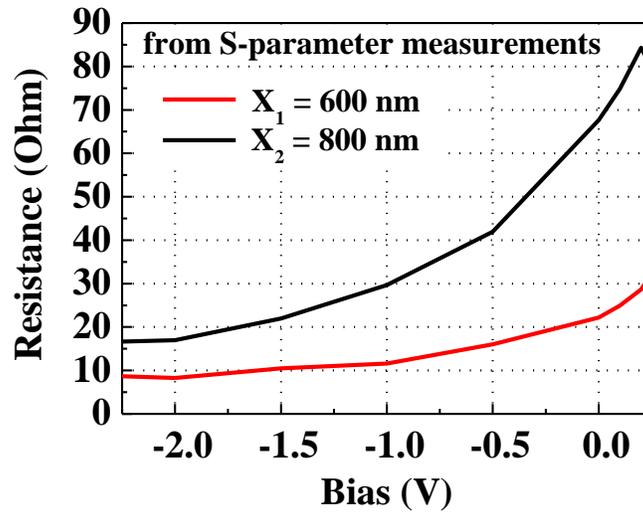
Fig. 6: Resistance of two diodes with different width "X", extracted from small signal measurements.

If these values are taken into account for the estimation of the cutoff frequency f_C, an improvement of a factor of two is obtained by a reduction of the SiN-pedestal width "X". The capacitance, resistance and resulting cutoff frequency values at 0 V are summarized in Table 1.

TABLE 1: DATA EXTRACTED FROM SMALL SIGNAL MEASUREMENTS AT ZERO-BIAS.

Diode	R (Ohm)	C (fF)	f_C (GHz)
X_1 = 600 nm	22	17	425
X_2 = 800 nm	68	11.5	203

Note that these values basically result from diode layouts formerly optimized for high-performance opto-electrical functionality. The lengths of the diodes (along the light incidence direction) and the SiN-pedestal widths are optimized for high bandwidths and responsivities.

A comparison to the SBD available in IHP's H-technology family proves a very similar cutoff-frequency performance, but, attributed to the p-i-n diode structure, at much lower leakage currents under reverse bias conditions.

In order to perform additional investigations on germanium p-i-n diodes, the frequency dependency of the insertion loss and isolation were estimated out of small signal measurements, conducted for both diodes X_1 and X_2, as presented in Fig. 7.
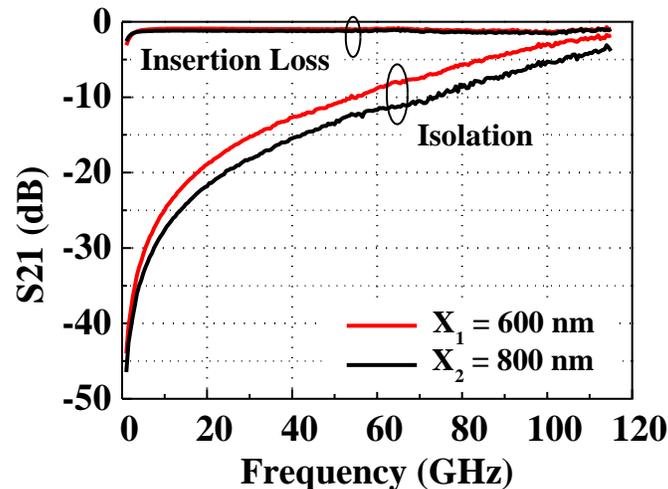

Fig. 7: Insertion Loss and Isolation estimated from small signal measurements for both diodes X_1 and X_2.

Whereas the insertion loss is, as favored, rather flat over the whole frequency range, the isolation shows a strong frequency dependency. For the existing diodes an isolation of -15 dB is only reached up to about 30 GHz, which we account on the disadvantageous design with respect to RF. As seen from Fig. 8, for the diode with X_1 = 600 nm distance of the metal pads of the anode and cathode is only about 1.2 µm over a length of about 20 µm, which results most probably in the relative poor isolation properties by coupling of the RF signal.

In order to improve the isolation and thus extending the frequency range of the germanium diode, this effect can, most probably, be reduced in future designs, in particular by optimizations in the design of the metal lines.
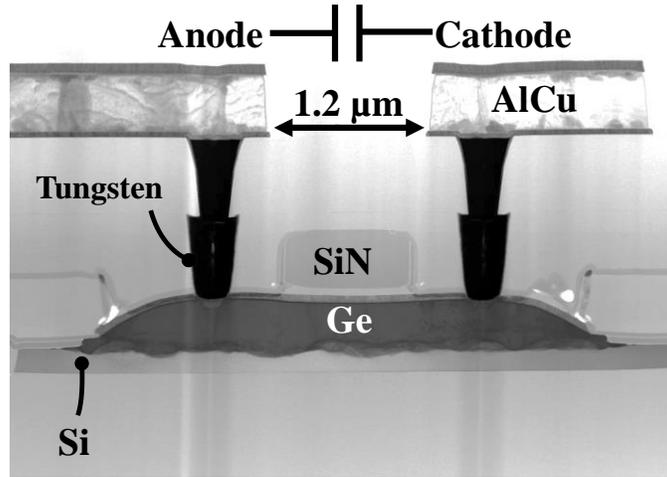

Fig. 8: TEM cross section of lateral germanium p-i-n diode: capacitive coupling between anode and cathode owed to improper RF design.

Fig. 9 proves good matching between the reflection estimated from small-signal measurements (S11) and simulated data. Over the whole frequency range the curves stay well below -20 dB, which is sufficiently low for most applications.
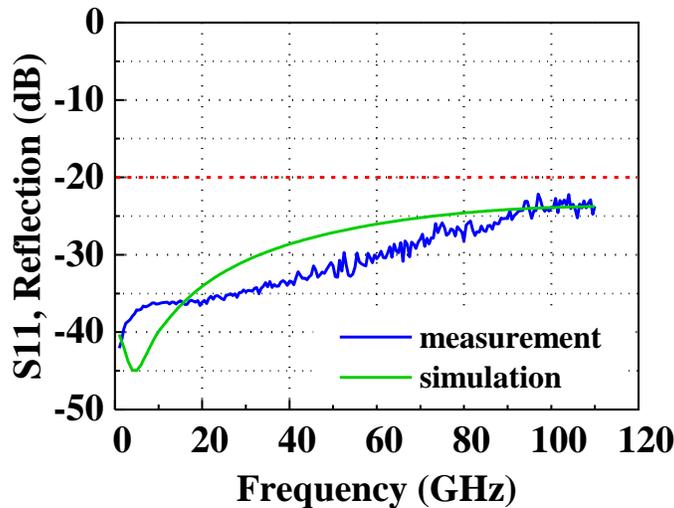

Fig. 9: Simulated and measured reflection (estimated from small signal measurements).

V. SUMMARY AND CONCLUSIONS

A germanium p-i-n diode from a photonic BiCMOS technology was presented, which is suited for side-use in electronic applications too. The presented results indicate that there is room for further improvements by reconsidering the design of the diodes for purely electrical side-use, in particular by scaling the length and width of the SiN-pedestal but also the RF design of the metal lines.

Enabled by the fact that both diode construction types solely result from layout variations, the diodes for electrical side-use can be optimized widely independent from the diodes optimized for best photo detector performance.

The side-use of the Ge p-i-n diodes may allow the replacement of the existing Schottky-barrier diodes available in the same process or potentially enable for switching RF signals without the need for MEMS.

REFERENCES

[1]   N. B. Feilchenfeld et al., "An integrated silicon photonics technology for O-band datacom," in 2015 IEEE International Electron Devices Meeting (IEDM), p. 25.7.1.

[2]   D. Knoll et al., "High-Performance Photonic BiCMOS Process for the Fabrication of High-Bandwidth Electronic-Photonic Integrated Circuits," in 2015 IEEE International Electron Devices Meeting (IEDM), 2015, pp. 402–405.

[3]   R. Ding et al., "100-Gb/s NRZ optical transceiver analog front-end in 130-nm SiGe BiCMOS," in 2014 IEEE Optical Interconnects Conference (OI), 2014, pp. 113–114.

[4]   J. Prades et al., "High speed phase modulator driver unit in 55 nm SiGe BiCMOS for a single-channel 100 Gb/s NRZ silicon photonic modulator," in 2015 10th European Microwave Integrated Circuits Conference (EuMIC), 2015, pp. 341–344.

[5]   D. Knoll et al., "High-performance BiCMOS Si photonics platform," in 2015 IEEE Bipolar/BiCMOS Circuits and Technology Meeting - BCTM, 2015, pp. 88–96.

[6]   S. Lischke et al., "High bandwidth, high responsivity waveguide-coupled germanium p-i-n photodiode," Optics express, vol. 23, no. 21, pp. 27213–27220, 2015.

[7]   D. Knoll et al., "Substrate Design and Thermal Budget Tuning for Integration of Photonic Components in a High-Performance SiGe: C BiCMOS Process," ECS Transactions, vol. 50, no. 9, pp. 297–303, 2012.

[8]   D. Knoll et al., "Monolithically Integrated 25Gbit/sec Receiver for 1.55µm in Photonic BiCMOS Technology," in Optical Fiber Communication Conference (OFC), 2014, p. Th4C.4.

[9]   A. Awny et al., "A 40 Gb/s Monolithically Integrated Linear Photonic Receiver in a 0.25µm BiCMOS SiGe:C Technology," IEEE Microw. Wireless Compon. Lett, vol. 25, no. 7, pp. 469–471, 2015.

[10] G. Winzer et al., "Monolithic photonic-electronic QPSK receiver for 28Gbaud," in Optical Fiber Communication Conference (OFC), 2015, p. M3C.4.

[11] D. Petousi et al., "Monolithic Photonic BiCMOS Sub-System Comprising MZM and Segmented Driver with 13 dB ER at 28 Gb/s," Proc. CLEO, San Jose (2016)..

[12] S. Lischke et al., "Photonic BiCMOS Technology –Enabler for Si-Based, Monolithically Integrated Transceivers Towards 400 Gbps," in press.

[13] S. Lischke et al., "High-speed, waveguide Ge PIN photodiodes for a photonic BiCMOS process," in 2014 IEEE Bipolar/BiCMOS Circuits and Technology Meeting - BCTM, 2014, pp. 29–32.

[14] S. Lischke et al., "Design Effects on the Performance of High-Speed Ge Photo Detectors," in press.